Theor Appl Climatol (2012) 110:373–384
DOI 10.1007/s00704-012-0631-0

ORIGINAL PAPER

Spatial and temporal variability of urban tree canopy temperature during summer 2010 in Berlin, Germany

Fred Meier · Dieter Scherer

Received: 4 January 2011 / Accepted: 8 March 2012 / Published online: 29 March 2012

Abstract Trees form a significant part of the urban vegetation. Their meteorological and climatological effects at all scales in urban environments make them a flexible tool for creating a landscape oriented to the needs of an urban dweller. This study aims at quantifying the spatio-temporal patterns of canopy temperature (T_C) and canopy-to-air temperature difference (ΔT_C) in relation to meteorological conditions and tree-specific (physiological) and urban site-specific characteristics. We observed T_C and ΔT_C of 67 urban trees (18 species) using a high-resolution thermal-infrared (TIR) camera and meteorological measurements in the city of Berlin, Germany. TIR images were recorded at 1-min intervals over a period of 2 months from 1st July to 31st August 2010. The results showed that ΔT_C depends on tree species, leaf size and fraction of impervious surfaces. Average canopy temperature was nearly equal to air temperature. Species-specific maximum ΔT_C varied between 1.9±0.3 K (*Populus nigra*), 2.9±0.3 K (*Quercus robur*), 3.2±0.5 K (*Fagus sylvatica*), 3.9±1.0 K (*Platanus acerifolia*), 4.6±0.2 K (*Acer pseudoplatanus*), 5.0±0.5 K (*A. platanoides*) and 5.6±1.1 K (*A. campestre*). We analysed ΔT_C for a hot and dry period (A) and a warm and wet period (B). The range of species-specific ΔT_C at noon was nearly equal, i.e. 4.4 K for period A and 4.2 K for period B. Trees surrounded by high fraction of impervious surfaces showed consistently higher ΔT_C. Knowledge of species-specific canopy temperature and the impacts of urban structures are essential in order to optimise the benefits from trees in cities. However, comprehensive evaluation and optimisation should take the full range of climatological effects into account.

F. Meier (✉) · D. Scherer
Department of Ecology, Technische Universität Berlin,
Rothenburgstraße 12,
12165 Berlin, Germany
e-mail: fred.meier@tu-berlin.de

D. Scherer
e-mail: dieter.scherer@tu-berlin.de

1 Introduction

From previous studies about urban vegetation and in particular urban trees, we know that trees produce distinct meteorological and climatological effects at all scales in urban environments (Heisler 1986; Oke 1989; Voogt and Oke 1997). This includes the influence of tree cover on the local-scale surface energy balance (Grimmond et al. 1996) and the reduction of canopy air temperature in comparison to the built environment by evapotranspiration and shadowing. However, the cooling effect differs from site to site and during the course of a day (Souch and Souch 1993; Spronken-Smith and Oke 1998; Upmanis et al. 1998; Shashua-Bar and Hoffman 2000; Potchter et al. 2006; Bowler et al. 2010). Trees reduce surface temperatures of the near surroundings (Hoyano 1988; Robitu et al. 2006; Shashua-Bar et al. 2009; Meier et al. 2010) and the building energy use (Rosenfeld et al. 1995; Akbari et al. 2001), and help to improve human thermal comfort by modifying the human energy balance (Mayer and Höppe 1987; Brown and Gillespie 1990; Streiling and Matzarakis 2003; Thorsson et al. 2004; Gulyás et al. 2006). Trees also modify the wind field in street canyons. This is important in relation to dispersion processes of pollutants (Gromke and Ruck 2007; Litschke and Kuttler 2008).

However, there are only few studies regarding the spatial and temporal variation of canopy temperature of urban trees and their response to the urban environment (Montague and Kjelgren 2004; Mueller and Day 2005). According to previous field studies, urban vegetative evapotranspiration is affected by advection and edge effects, i.e. the oasis or clothesline effect because of strong surface heterogeneity in urban environments (Oke 1979; Hagishima et al. 2007). The experiment of Heilman et al. (1989) shows that presence of walls changes the water consumption of adjacent shrubs. Kjelgren and Montague (1998) reveal that trees over asphalt have higher leaf temperatures than those over natural surfaces. This results in higher water loss or the closing of stomata depending on tree species. A study from Basel, Switzerland, based on thermal-infrared (TIR) imagery obtained during a helicopter flight shows that tree canopy temperatures at noon are species-specific and depend on location, leaf size and stomatal conductance (Leuzinger et al. 2010). There have been no studies which quantify canopy temperature over a wide range of species, sites and atmospheric conditions in an urban environment, beyond those that report temporal dynamics of several individual trees at different sites (e.g. Montague and Kjelgren 2004) or one-time canopy temperature of more than 400 trees (Leuzinger et al. 2010).

The objective of this study is to estimate spatio-temporal variability of canopy temperature (T_C) and canopy-to-air temperature difference ($\Delta T_C = T_C - T_a$) of individual trees in an urban environment. We aim at quantifying the spatio-temporal patterns of T_C and ΔT_C in relation to meteorological conditions and tree-specific (physiological) and site-specific characteristics. State-of-the-art TIR cameras mounted on towers or high-rise buildings allow a simultaneous sampling of spatial and temporal changes of canopy temperatures by recording time series of thermal images. We will refer to this as time-sequential thermography (TST, Hoyano et al. 1999). The obtained TST data cover a period of 62 days from 1st July to 31st August 2010. In the long-term perspective, we will collect climate data of species-specific canopy temperature and ΔT_C in an urban environment in order to compare different years. In detail, we address the following questions:

1) Are there differences in terms of ΔT_C between and within the observed crowns in our study area, and if so, how is the magnitude during a diurnal cycle?
2) To what extent ΔT_C varies due to different atmospheric and moisture conditions, species-specific variables as well as site-specific conditions?

In the next section, we describe the study site, our experimental setup, the pre-processing steps of TST data and the tree survey. Section 3 presents the observed spatio-temporal patterns of ΔT_C and their relation to meteorological conditions, species-specific variables and site-specific conditions. The "Discussion" section gives answers to the above-mentioned questions under consideration of previous studies.

2 Materials and methods

2.1 Study site and experimental setup

The study was conducted in the city of Berlin, Germany (52°27′N, 13°19′E) in the south-western Steglitz-Zehlendorf district. During the experiment, the site was characterised by a high amount of vegetation, five to six-storey block development with courtyards and mature trees, low-rise residential houses, street trees, one park with mature trees and a playground, villas with gardens and one high-rise building. The study was conducted under the umbrella of the urban climate research program 'Energy eXchange and Climates of Urban Structures and Environments' (EXCUSE) that focuses on quantification of energy, momentum and mass exchange processes in the urban boundary layer. The EXCUSE research infrastructure includes a measurement platform on top of the high-rise building and comprises a TIR camera system (7.5–14.0 μm, 320×240 pixels, VarioCAM® head, InfraTec GmbH). The fixed field of view (FOV) of the TIR camera covers an area of approximately 0.3 km^2. Within the FOV, a meteorological station measures air temperature T_a, relative humidity RH (HMP45A, Vaisala) and downward short-wave radiation $^{\downarrow}E_{SW}$ (Starpyranometer 8101, Schenk GmbH) at a height of 22.5 m above ground, whereas wind velocity and wind direction measurements are conducted at a height of 23 m above ground using a cup anemometer and vane (Lambrecht GmbH). A tipping-bucket rain gauge measures precipitation at 0.1-mm resolution. The position of the meteorological station is depicted in Fig. 1.

2.2 Thermal remote sensing data

The TIR camera was oriented towards northwest (325°) and inclined by 59° from the nadir angle. Therefore, main parts of the observed crowns were oriented towards southeast. We expect different T_C for unseen areas of the crown resulting from effective thermal anisotropy (Lagouarde et al. 2000; Voogt and Oke 2003). Hence, we analysed a directional canopy temperature and not the complete canopy temperature, which represents the three-dimensional (3-D) crown surface (Voogt and Oke 1997).

TIR images were recorded at 1-min intervals. The pre-processing of TIR images comprised four steps. At first, radiance was converted into brightness temperature T_b using firmware calibration parameters and case temperature under the assumption that the surface is a Lambertian blackbody. The wide-angle lens produced radiometric and geometric distortions, which were corrected in steps two and three. Furthermore, an atmospheric correction was applied to account for spatial variability of line-of-sight (LOS) geometry due to the oblique view and the 3-D character of the examined urban environment. The reader is referred to the work of Meier et al.

Fig. 1 The field of view (FOV) and viewing direction (northwest) of the TIR camera. The symbols indicate tree genus. Numerals are used to indicate individual trees in the text

(2011) for further details on radiometric, geometric and atmospheric corrections. We utilised data of the WMO station 10381 Berlin-Dahlem in order to make an atmospheric correction for cloudy conditions. All TIR data collected under rainy conditions and cloud heights below 330 m were not used. Finally, 63180 TIR images (2106 half-hourly averages) were used for the analysis. This corresponded to 71 % of the two-month measurement period.

We applied the Stefan–Boltzmann law (δ=Stefan–Boltzmann constant) assuming an emissivity (ε) of 0.97 for the canopy surface (Campbell and Norman 1998) in order to compute T_C. Further, we account for reflected downward long-wave radiation (${}^{\downarrow}E_{LW}$) measured on top of the high-rise building (Eq. 1). A detailed consideration of reflected long-wave radiation originated from other parts than the sky (walls, roofs and ground surfaces) was not yet possible due to unknown view factors of tree pixels and not TIR-scanned surrounding surfaces.

$$T_b^4 \cdot \delta = T_C^4 \cdot \varepsilon \cdot \delta + (1-\varepsilon) \cdot {}^{\downarrow}E_{LW} \quad (1)$$

The sensor-target distances were between 150 and 550 m. Therefore, the spatial resolutions of tree pixels were between 0.5 and 2 m. This spatial resolution exceeds typical leaf size values, and in fact T_C is a spatial integral over a lot of leaves and partly branches.

We calculated the spatial median of all T_C corresponding to an individual tree crown in order to quantify the canopy temperature of a single tree. The temperature range within the crown was defined as the difference between the 95th and 5th percentiles of T_C. Although T_a was measured 22.5 m above ground, we expect spatial variability of T_a at this height within the FOV. This aspect was beyond the scope of the study and was not considered in the calculation of ΔT_C.

2.3 Tree data

We selected 67 individual trees and compiled a crown mask based on photographs from the high-rise building and TIR images. Each crown could be clearly separated from other surrounding surfaces. Figure 1 shows the FOV of the TIR camera and all selected crowns, which represent approximately 40 % of all trees inside the FOV. Among these, we found *Acer platanoides*, *A. pseudoplatanus*, *A. campestre*, *Fagus sylvatica*, *Populus nigra*, *Platanus acerifolia, Quercus robur*, *Tilia* spp. and various conifers (e.g. *Taxus baccata*, *Pinus sylvestris*, *Larix decidua, Abies procera*). For 41 broadleaf trees, we measured the leaf size of 20–50 leaves per tree using a leaf area meter (Li-Cor Model 3100). In order to estimate the influence of tree-specific location within the city, we computed the mean fraction of impervious surfaces (FIS) around the trunk in a square of 50×50 m. This area was oriented towards southeast taking into account the viewing direction of the camera, i.e. 10 m towards north and west and 40 m towards south and east, respectively. For this purpose, we used the 'Impervious Soil Coverage' map of Berlin that is available in a 2.5-m raster format (Senate Department for Urban Development 2007). One important driver of T_C is the stomatal conductance (g_s) (Jones 1992). The tree-specific stomatal conductance was not measured in our study.

However, there are differences between species regarding the maximum g_s (Körner et al. 1979). We made a literature survey in order to have an estimation of the maximum g_s values for the investigated species. Species-specific tree data are summarised in Table 1.

3 Results

This section starts with an overview of spatio-temporal patterns showing the spatial distribution of minimum, mean and maximum ΔT_C. Then we present the influence of atmospheric conditions and tree-specific and site-specific parameters on the spatio-temporal variability of ΔT_C. All time specifications refer to Central European Time (CET).

3.1 Spatio-temporal patterns

In addition to the ΔT_C patterns, we present spatio-temporal patterns of the surface-to-air temperature difference (ΔT) for every pixel of the whole FOV based on Eq. 1 to facilitate interpretability. Trees on the city square showed the highest mean ΔT_C. They reached values up to 0.9 K (Fig. 2b, lower right corner). The average canopy temperatures of park trees were close to air temperature. Some individuals, for instance *P. nigra* (No. 43 in Fig. 1), reached values up to −0.5 K. Only trees and lawn surfaces showed negative ΔT values in

Table 1 Number of replicates and in parenthesis number of individuals, where leaf size was measured, number of thermal-infrared (TIR) pixels (i) and species-specific values of leaf size and standard deviation (where applicable), fraction of impervious surfaces (FIS) and standard deviation (where applicable)

Species	Species ID	Number	*i*	Leaf size (cm^2)	FIS (%)	g_s ($mm\ s^{-1}$)
Abies procera (Noble fir)	S1	1 (0)	213	–	40	2.7[a]
Acer campestre (Field maple)	S2	2 (1)	365	29	95±7	2.0[b]
Acer negundo (Maple ash)	S3	1 (0)	260	–	45	5.6[c]
Acer platanoides (Norway maple)	S4	9 (7)	1601	84±24	41±28	3.2[d]
Acer pseudoplatanus (Sycamore maple)	S5	5 (4)	980	93±15	37±19	7.8[e]
Fagus sylvatica (Beech)	S6	12 (11)	1942	31±8	33±23	6.1[f]
Larix decidua (European larch)	S7	1 (0)	83	–	35	5.8[g]
Pinus nigra (Black pine)	S8	2 (0)	67	–	60±0	2.2[h]
Pinus sylvestris (Scots pine)	S9	1 (0)	53	–	67	6.7[i]
Pinus wallichiana (Blue pine)	S10	2 (0)	174	–	31±8	–
Platanus acerifolia (London plane)	S11	5 (0)	697	–	69±34	5.9[d]
Populus nigra (Black poplar)	S12	3 (3)	219	27±10	32±2	8.9[j]
Quercus robur (Oak)	S13	9 (9)	2602	34±8	48±30	11.2[e]
Taxus baccata (Yew)	S14	4 (0)	376	–	75±28	2.1[k]
Thuja occidentales (whitecedar)	S15	1 (0)	102	–	11	3.7[k]
Tilia cordata (Littleleaf linden)	S16	2 (2)	269	37±6	30±16	4.3[d]
Tilia x europaea (Common linden)	S17	3 (1)	222	33.0	55±29	–
Tilia platyphyllos (Bigleaf linden)	S18	4 (2)	399	45±9	51±31	2.8[d]

Maximum stomatal conductance (g_s) is cited from the indicated reference

[a] Running (1976)

[b] Elias (1979)

[c] Foster (1992)

[d] Leuzinger et al. (2010)

[e] Morecroft and Roberts (1999)

[f] Leuzinger and Körner (2007)

[g] Handa et al. (2005)

[h] Lebourgeois et al. (1998)

[i] Sandford and Jarvis (1986)

[j] Fortunati et al. (2008)

[k] Lusk et al. (2003)

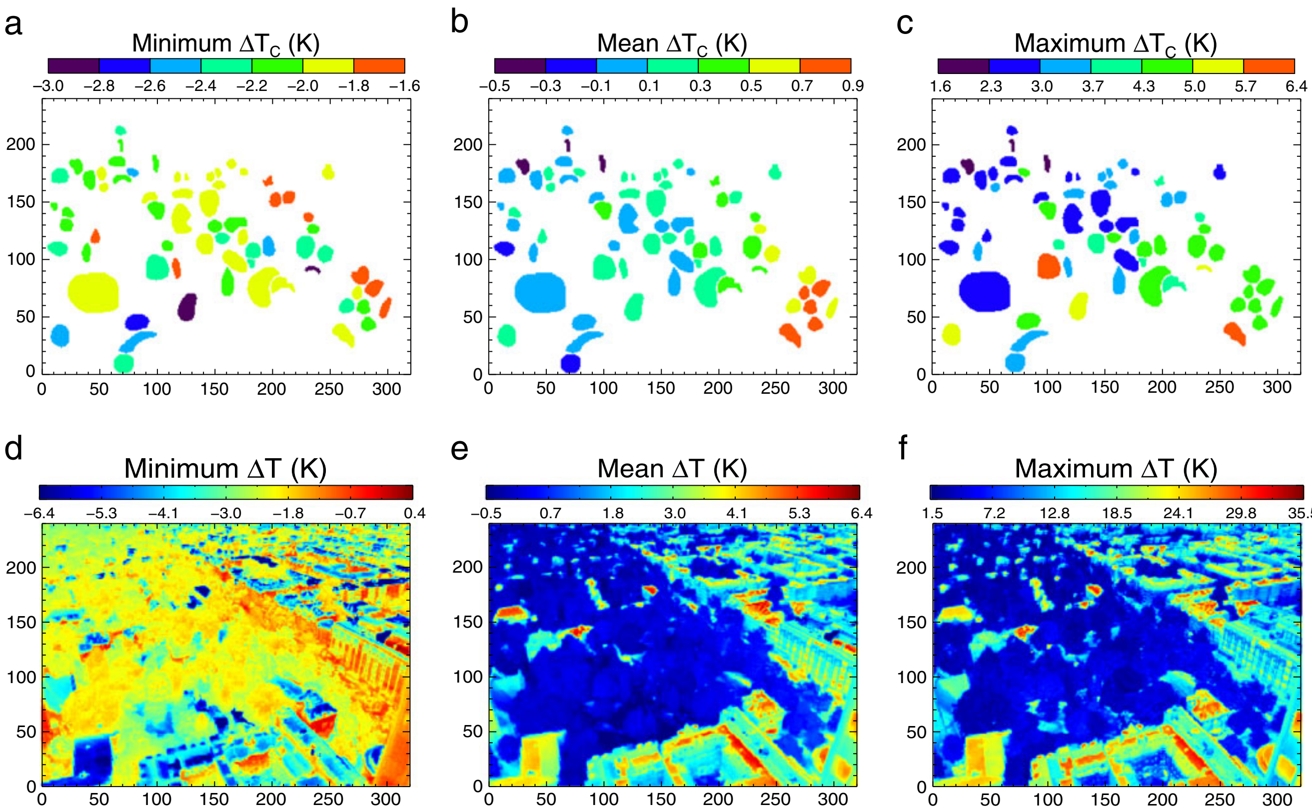

Fig. 2 Spatio-temporal patterns of **a** minimum, **b** mean and **c** maximum canopy-to-air temperature difference (ΔT_C), as well as **d** minimum, **e** mean and **f** maximum surface-to-air temperature difference (ΔT). The *x*- and *y*-axes values are the column and row index of each pixel

the mean pattern. All other urban surfaces showed positive ΔT values.

The minimum ΔT_C ranged from −3.0 to −1.6 K (Fig. 2a). Trees along the road were relatively warm in comparison to park trees. Roofs of buildings and lawns showed the lowest minimum ΔT values. They were up to 5–6 K cooler than air temperature (Fig. 2d).

The maximum ΔT_C ranged from 1.6 to 6.4 K (Fig. 2c). Trees No. 2 (*A. campestre*) and No. 10 (*A. platanoides*) reached the highest maximum ΔT_C values. Two-thirds of the 67 trees reached their maximum ΔT_C between 0900 and 1100 hours. Roofs of buildings showed maximum surface-to-air temperature differences of more than 30 K (Fig. 2f).

3.2 Influence of weather conditions

3.2.1 Meteorological conditions during the study period

Table 2 summarises meteorological conditions during June, July and August 2010 and the corresponding long-term values (standard period 1961–1990, 2 m above ground) recorded at the climate station Berlin-Dahlem, Albrecht-

Table 2 Monthly means of air temperature (T_a) and vapour pressure deficit (VPD), monthly sums of downward short-wave radiation (${}^{\downarrow}E_{SW}$) and precipitation in 2010 in comparison to climate data for the 1961–1990 period measured at the climate station Berlin-Dahlem, Albrecht-Thaer-Weg (Chmielewski and Köhn 1999)

	T_a (°C)		${}^{\downarrow}E_{SW}$ (MJ m^{-2})		VPD (hPa)		Precipitation (mm)	
	2010	1961–1990	2010	1961–1990	2010	1961–1990	2010	1961–1990
June	18.4	17.1	652.2	532.7	10.1	7.0	6.4	70.0
July	23.1	18.5	660.6	521.5	14.9	7.5	55.2	53.0
August	18.5	18.0	421.7	446.4	6.5	6.7	138.3	64.0

Thaer-Weg (Chmielewski and Köhn 1999), which is situated at a distance of 1.5 km to the northwest of the study site. The June values are included in order to show the very low amount of precipitation (6.4 mm) before the study period. During July, T_a and VPD exceeded the long-term means by about 4.6 K and 7.4 hPa respectively.

Figure 3 shows daily means of T_a, VPD and daily sums of precipitation. The daily minimum, maximum and mean values of ΔT_C are only depicted for days with more than 75 % data availability. Especially July was very hot and dry leading to persistent high values of T_a and VPD. On July 11, the average T_a was higher than 30 °C, and VPD reached 27 hPa. The daily means of ΔT_C ranged between −0.4 and 0.9 K. The maximum ΔT_C was higher than 5 K for 14 days in July and only for 5 days in August.

Due to the different weather conditions, we decided to analyse two representative periods in detail. We made a distinction between the hot period with dry soils (period A, 10th July 2010) and the warm period with replenished soils (period B, 29th July 2010). The grey bands in Fig. 3 show these 2 days. The sum of downward short-wave radiation was similar on both days, i.e. 26.5 MJ m^{-2} during period A and 26.1 MJ m^{-2} during period B.

3.2.2 Diurnal course and histogram of canopy temperatures

The maximum range (maximum T_C−minimum T_C) was 5.2 K for period A and 5.4 K for period B. Although maximum variability was equal in both cases, it was observed at different times, i.e. at 1300 hours for period A and at 0930 hours for period B. In both periods, maximum canopy temperatures were reached before maximum air temperatures.

The grey box plots (Fig. 4) of the hot and dry period (A) reveal that nearly all tree crowns were warmer than air temperature during daytime. Mean ΔT_C was positive between 0630 and 2030 hours. The white box plots (Fig. 4) of the warm and wet period (B) show that several tree crowns were cooler than air temperature during the day. In both periods, the mean ΔT_C values were negative during the night.

The difference between both periods in terms of ΔT_C is clearly visible in the histograms presented in Fig. 5. The histogram of period A is shifted to higher values and shows a bimodal distribution. Average ΔT_C was higher during the hot and dry period (mean 0.9 K, median 0.7 K) than during the warm and wet period (mean 0.1 K, median −0.3 K). Both distributions had a positive skewness.

3.3 Species-specific temperature patterns

Table 2 summarises the observed temperature patterns of all species. The average daily mean ΔT_C of all species was slightly above air temperature (0.2 K). Only *P. nigra* was cooler than air temperature. All other species were on average warmer or equal to air temperature. *A. campestre* and *T. baccata* reached the highest average values of 0.7 K. Species-specific maximum ΔT_C varied between 1.9 and 5.6 K. The mean canopy temperature was between 22.3 and 23.4 °C. *A. platanoides*, *P. acerifolia* and *T. baccata* reached maximum T_C values of 40 °C. The average daily range within the crown was 0.8 K. Species-specific maximum temperature range within the crown was between 1.6 K (*P. sylvestris*) and 4.4 K (*A. pseudoplatanus*, *A. campestre*).

3.3.1 Comparison between period A and period B

For period B the magnitude and ascending order of daily mean ΔT_C corresponds to Table 3. During period A, all species had significantly higher daily mean and noon ΔT_C values (Fig. 6a, d). The largest temperature difference (period A−period B) of 0.9 K was observed for *L. decidua*, *Tilia x europaea*, *T. baccata* and *P. wallichiana*.

At night, species-specific range (maximum ΔT_C − minimum ΔT_C) was very low, i.e. 1.2 K for period A and 0.6 K

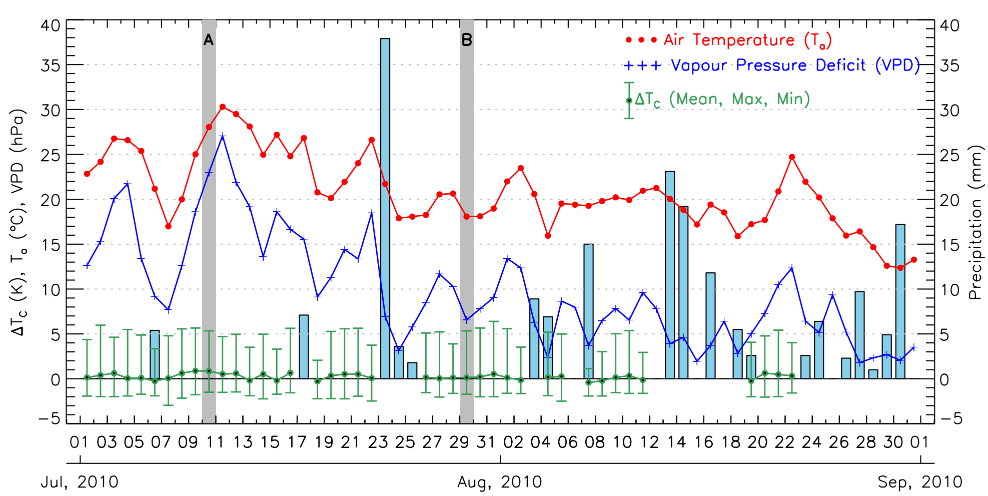

Fig. 3 Temporal variation of daily air temperature (T_a), vapour pressure deficit (VPD), precipitation and canopy-to-air temperature difference (ΔT_C). The *grey* bands indicate the hot and dry period A as well as the warm and wet period B

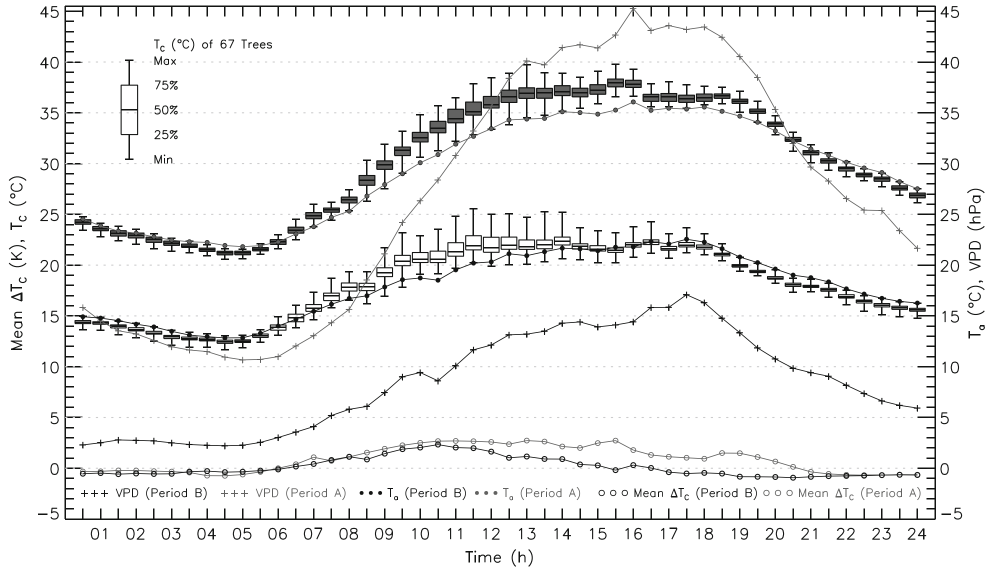

Fig. 4 Diurnal courses of mean canopy-to-air temperature difference (ΔT_C), canopy temperature (T_C) of 67 trees (*box plots*), air temperature (T_a) and vapour pressure deficit (VPD) for period A and B. *Grey* box plot represents data from period A

for period B, but interestingly *A. platanoides* and *A. pseudoplatanus* showed the lowest values in contrast to the daytime situation (Fig. 6c). The largest differences (period A−period B, nighttime ΔT_C) were observed for *T. baccata* (0.5 K), *A. campestre* (0.4 K) and *L. decidua* (0.4 K).

Furthermore, data from the noon situation was analysed, because we expect minimum influence of shadowing due to buildings and other objects at this time. While downward short-wave radiation was similar at noon (830 Wm^{-2}), a higher T_a was observed during period A (34.4 °C vs. 21.1 °C). The species-specific range at noon was 4.4 K for period A and 4.2 K for period B. *P. nigra* showed the lowest values during both periods. *A. campestre* showed the highest ΔT_C, but only a moderate temperature difference of 0.9 K between both periods at noon. The largest temperature differences were observed for *P. wallichiana* (1.9 K), *Tilia x europaea* (1.8 K) and *A. negundo* (1.5 K).

At noon the range of T_C within the crown was higher for deciduous trees than for conifers (Fig. 6b). All species except *P. nigra* (−0.1 K) showed an increase in the range of T_C within the crown of up to 0.8 K for *F. sylvatica*. The mean range of T_C within the crown at noon was 1.1 K for the warm and wet period and 1.6 K for the hot and dry period.

3.3.2 Relation between leaf size and canopy temperature

The size of the examined tree-specific leaves was between 19 cm^2 (*P. nigra*, No. 43) and 111 cm^2 (*A. pseudoplatanus*, No. 15). *A. platanoides* and *A. pseudoplatanus* showed the highest standard deviation (see also Table 1). Figure 7 shows

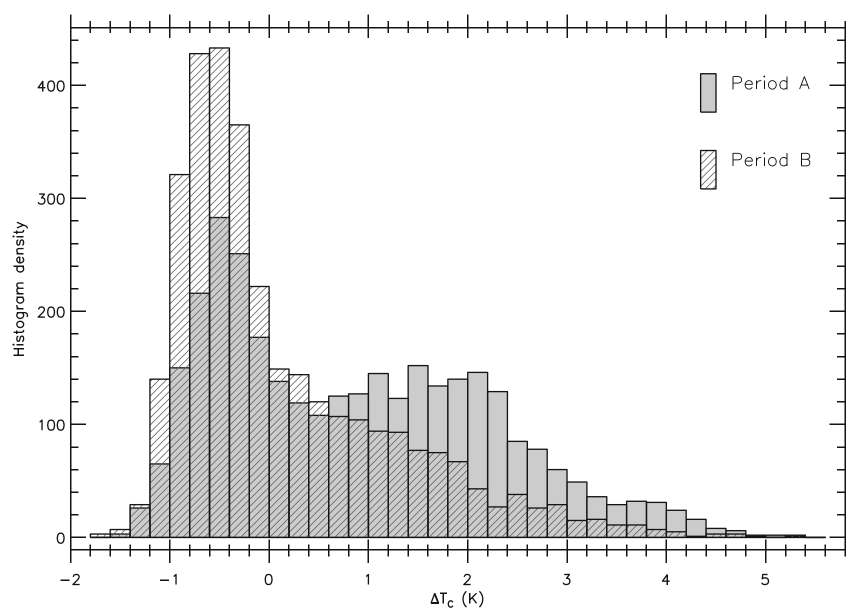

Fig. 5 Histogram of canopy-to-air temperature difference (ΔT_C) during periods A and B

Table 3 Species-specific values ± standard deviation (where applicable) of canopy temperature (T_C), canopy-to-air temperature difference (ΔT_C) and temperature range within the crown, sorted by increasing average daily mean of ΔT_C (only days with more than 75 % data availability)

Species	Mean ΔT_C (K)	Max ΔT_C (K)	Min ΔT_C (K)	Mean T_C (°C)	Max T_C (°C)	Mean range (K)	Max range (K)
Populus nigra	−0.4±0.1	1.9±0.3	−2.1±0.0	22.3±0.1	37.0±0.1	0.8±0.1	3.5±1.2
Acer negundo	0.0	3.5	−2.5	22.7	38.4	0.6	2.5
Quercus robur	0.0±0.1	2.9±0.3	−1.9±0.2	22.7±0.1	38.4±0.5	0.8±0.2	3.2±1.0
Abies procera	0.1	3.4	−2.0	22.8	37.8	0.8	2.7
Fagus sylvatica	0.1±0.1	3.2±0.5	−2.0±0.2	22.8±0.1	38.5±0.3	0.8±0.2	3.4±1.6
Tilia cordata	0.1±0.1	2.9±0.4	−2.1±0.3	22.8±0.1	37.7±0.1	0.7±0.1	2.5±0.1
Larix decidua	0.2	2.5	−1.9	22.9	38.0	0.5	1.8
Pinus sylvestris	0.2	3.1	−2.0	22.9	38.5	0.5	1.6
Thuja occidentales	0.2	3.1	−1.7	23.0	37.7	0.6	2.4
Pinus nigra	0.2±0.0	2.6±0.0	−1.8±0.1	22.9±0.0	37.9±0.0	0.5±0.1	3.7±0.5
Pinus wallichiana	0.2±0.1	3.2±0.5	−1.9±0.3	22.9±0.1	38.7±0.1	0.7±0.2	2.7±0.3
Tilia platyphyllos	0.2±0.1	3.2±0.5	−2.0±0.1	22.9±0.1	38.7±0.4	0.8±0.2	3.5±1.4
Acer pseudoplatanus	0.3±0.1	4.6±0.2	−2.3±0.3	23.0±0.1	39.4±0.7	1.0±0.1	4.4±0.5
Tilia x europaea	0.4±0.0	3.7±0.3	−1.7±0.1	23.1±0.0	39.1±0.2	0.9±0.1	3.9±0.7
Acer platanoides	0.4±0.1	5.0±0.5	−2.4±0.3	23.1±0.1	40.0±0.8	1.0±0.2	4.0±0.5
Platanus acerifolia	0.5±0.4	3.9±1.0	−1.8±0.2	23.2±0.4	40.1±1.0	1.1±0.5	3.3±1.6
Acer campestre	0.7±0.2	5.6±1.1	−2.1±0.2	23.4±0.2	39.7±0.0	1.0±0.2	4.4±0.9
Taxus baccata	0.7±0.3	4.4±0.5	−2.1±0.2	23.4±0.3	40.0±0.5	0.7±0.1	3.0±0.4
Mean	0.2±0.4	3.6±1.0	−2.0±0.3	22.9±0.3	38.3±0.8	0.8±0.2	3.4±1.1

that trees with smaller leaves had lower ΔT_C during daytime for both periods. The leaf size of *A. campestre* (No. 2) is small in comparison to the other *Acer* trees, but this individual showed the highest ΔT_C during daytime in both periods. During the night, small leaves were slightly warmer than big leaves, but regression analysis yielded a very low correlation between these two parameters (not shown, period A: $r^2=0.11$, $p=0.04$, period B: $r^2=0.26$, $p<0.01$).

3.4 Influence of site-specific characteristics

The spatio-temporal patterns of ΔT_C presented in Fig. 2 already show a relation between the specific urban location of the tree and its thermal behaviour. To investigate this relation, we used the species-specific FIS around each tree as a quantitative descriptor representing the influence of urban structures on its thermal behaviour. The FIS values were between 11 % (*Thuja occidentales*) and 95 % (*A. campestre*). Figure 8 shows that species surrounded by a higher fraction of impervious surfaces had higher daily mean ΔT_C. This relation was slightly stronger for the hot and dry period regarding the linear correlation coefficients r^2 (A: 0.38 vs. B: 0.36).

4 Discussion

The spatial and temporal resolution of the presented urban surface temperature in combination with meteorological measurements allows analysing canopy-to-air temperature differences of individual trees belonging to 18 species. For the first time, half-hourly data spanning a period of 2 summer months could be presented. Average canopy temperature was nearly equal to air temperature. Therefore, it is possible to determine the average canopy temperature based on air temperature. This is helpful if canopy temperature is not explicitly measured or calculated by an energy balance approach. For instance, the SOLWEIG model (Lindberg and Grimmond 2011) uses this assumption for the simulation of spatial variations of 3-D radiation fluxes and mean radiant temperature. However, the assumption is questionable for a full description of a diurnal cycle and species-specific differences.

4.1 Variability of T_C within the crown

The maximum observed variability of T_C within the crown varied between 1.6 and 4.4 K. These differences could have an impact on the diversity of animal and plant communities in tree crowns. Broad-leaved deciduous trees showed higher values than conifers (Fig. 6b). Leuzinger and Körner (2007) report higher values for mature forest trees, i.e. between 6 and 11.8 K, although deciduous trees show also higher values than conifers. The different experimental set-up could have been the reason for these differences in magnitude. They mounted the TIR camera directly above the canopy resulting in a higher geometrical resolution, which

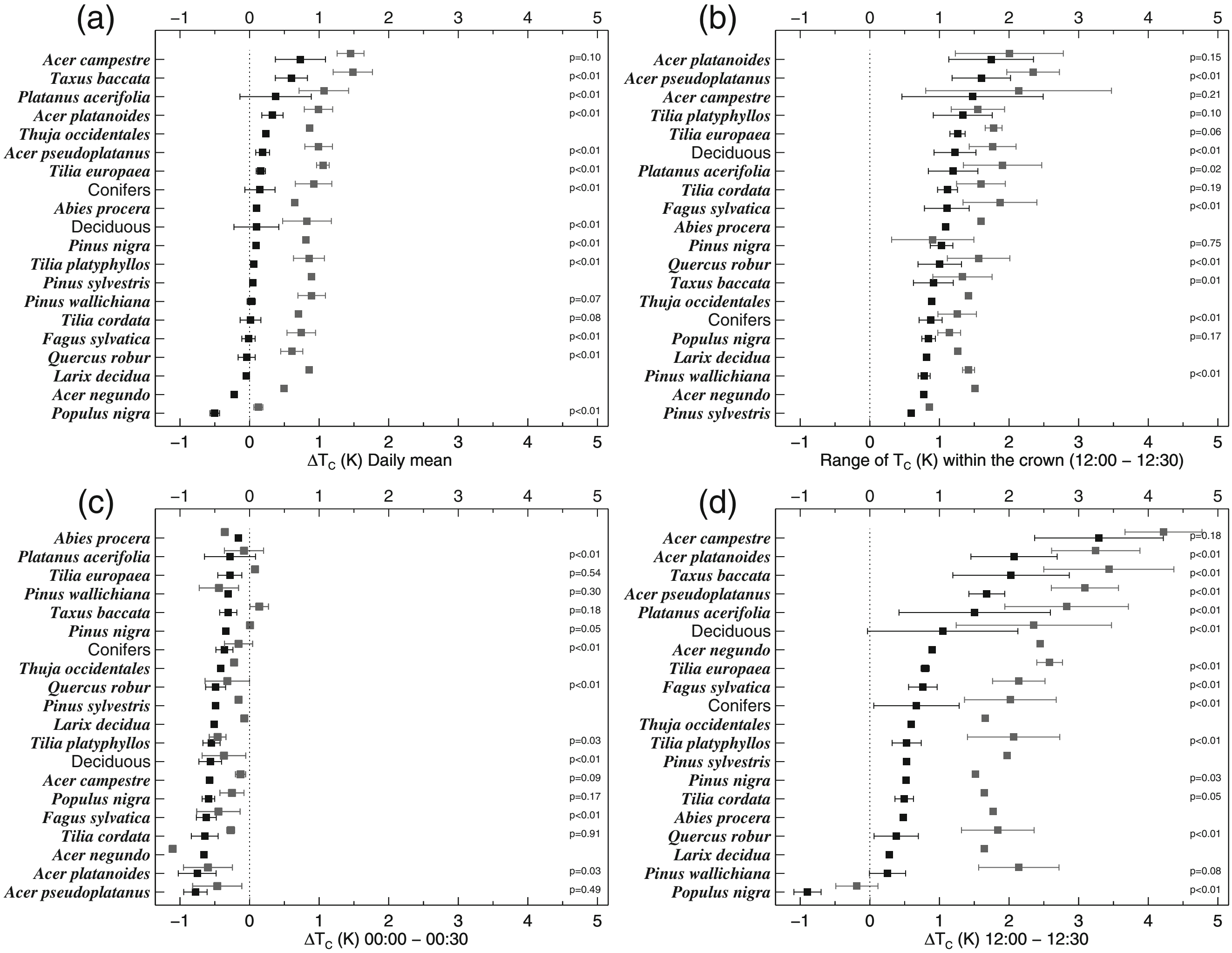

Fig. 6 Species-specific values ± standard deviation (where applicable) of **a** daily mean canopy-to-air temperature difference (ΔT_C), **b** temperature range within the crown at noon, **c** ΔT_C at midnight and **d** ΔT_C at noon. *Grey* symbols indicate data of period A, and *black* symbols indicate period B. The species were sorted using the values of period B. *p*-Values refer to *t*-tests of period A versus period B temperatures

provides more details of canopy structure like branching, leaf area density or sunlit and shadowed areas. The range of species-specific daily average ΔT_C corresponds to the magnitude of the mean temperature variability within the crowns (Table 2, 1.1 vs. 0.8 K). However, at noon the temperature variability among species was greater than variability within the crown (Fig. 6b, d).

It has been proposed that temperature variability within a canopy is a better indicator of plant water stress

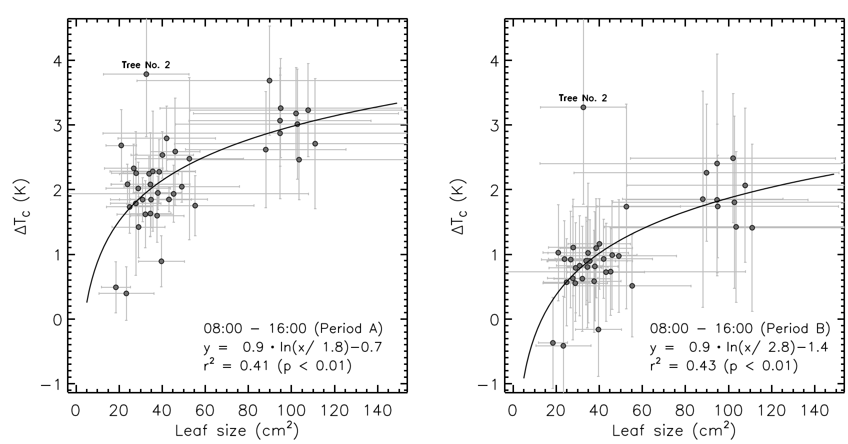

Fig. 7 Relation between leaf size and canopy-to-air temperature difference (ΔT_C) averaged for the daytime situation of period A (*left*) and period B (*right*). *Horizontal error bars* indicate ± standard deviation of leaf size. *Vertical error bars* indicate ± temporal standard deviation of ΔT_C between 0800 and 1600 hours

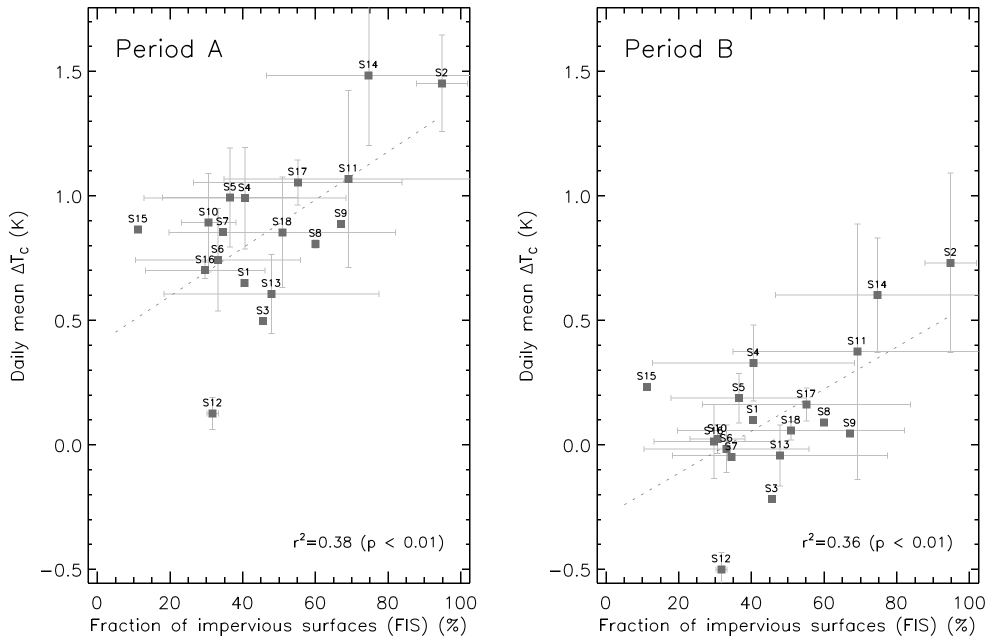

Fig. 8 Relation between fraction of impervious surfaces (FIS) and daily mean canopy-to-air temperature difference (ΔT_C) for period A (*left*) and period B (*right*). *Vertical error bars* indicate ± standard deviation of ΔT_C, and *horizontal error bars* indicate ± standard deviation of FIS within the species (where applicable)

than the average canopy temperature (Fuchs 1990). The observed increase of temperature variability within the crowns for period A (Fig. 6b) could be an indicator of plant water stress. However, buildings and isolated trees produce shadow patterns. We cannot neglect this influence, even if we have analysed temperature patterns at high sun elevations.

4.2 Variability of species-specific ΔT_C in the daytime

The observed differences between species can be explained with the help of species-specific stomatal conductance and leaf size (Table 1). *P. nigra* and *Q. robur* reach high stomatal conductance values. We expect high transpiration rates and lower ΔT_C for these tree species during ample water supply. The observed ΔT_C for these species (Table 2 and Fig. 6) confirm this. For the hot and dry period as well as during noon, we expect stomatal regulation of transpiration via stomatal closure. Leuzinger et al. (2010) present species-specific variations of ΔT_C based on calculations of the leaf energy balance under the assumption of decreasing g_s up to 20 % of maximum g_s. A comparison of these results with our observations, especially maximum ΔT_C, suggests that g_s did not decline below 50 %. This could indicate the presence of sufficient soil moisture and no severe water stress even during the hot and dry period. However, in order to confirm differences in stomatal regulation of transpiration, we need more information on the variation of tree-specific stomatal conductance.

The size and shape of leaves are important for heat loss by convection (Vogel 2009). These species-specific properties influence the heat and mass exchange between leaf and atmosphere (Schuepp 1993). As expected and previously shown (Leuzinger and Körner 2007; Leuzinger et al. 2010), trees with small and lobed leaves (e.g. *Q. robur*) as well as conifers (e.g. *L. decidua*, *P. sylvestris*, *P. wallichiana*) tend to reach lower temperatures. The thin flattened petioles of *P. nigra* cause the flutter of leaves even during low wind speed. This behaviour additionally reduces the boundary layer resistance and therefore leaf temperature (Grace 1978). Contrary to that, trees with large leaves tend to reach higher temperatures (e.g. *A. platanoides*, *A. pseudoplatanus*, *P. acerifolia*). In the study of Leuzinger et al. (2010), individuals of *A. platanoides* showed maximum ΔT_C of >5 K. This corresponds to our results (Fig. 2c and Table 2).

4.3 Variability of species-specific ΔT_C at night

Due to the reduced boundary layer resistance for smaller leaves, they tend to show higher temperatures than larger leaves in case of ΔT_C<0 as described in the example in Campbell and Norman (1998). This might be the reason for the observed temperature pattern during the night (Fig. 6c). Furthermore, if the TIR camera observes a relatively open crown, then we also measure radiation emitted from surfaces within the crown. These surfaces should have higher temperatures during the night because of the different long-wave radiation balance.

The crowns of trees No. 4 and No. 9 reach exactly the roof edges of an adjacent building. This might be influencing the cooling process of the crown, because roofs have the lowest surface temperature during nighttime (Fig. 2). Spronken-Smith and Oke (1998) analysed thermal imagery of urban parks and their surroundings, where roofs were also cooler than tree canopies during nighttime.

4.4 Spatial variability of ΔT_C

The influence of the tree-specific location within the city is superimposed onto the above-stated relation between leaf size and ΔT_C. The leaves of tree No. 2 are rather small (33 cm^2), but this tree is surrounded by a high fraction of impervious surfaces and reached the maximum ΔT_C during the study. Previous studies point out the effect of urban ground cover on tree microclimate (Whitlow et al. 1992) and leaf temperatures (Kjelgren and Montague 1998; Montague and Kjelgren 2004; Mueller and Day 2005). Our study confirms that trees over impervious surfaces exhibit consistently higher canopy temperatures due to interception of upward long-wave radiation from fabricated surfaces having higher surface temperatures. Higher leaf temperature enhances the leaf-to-air vapour pressure deficit and the relevance of stomatal control on transpiration (Kjelgren and Montague 1998; Celestian and Martin 2005). However, for short periods building shadows can reduce canopy temperature (Meier et al. 2010).

One frequently discussed way to reduce the radiative input in urban areas is the use of high albedo materials. This measure would decrease the emission of long-wave radiation, but would also increase the trees' absorption of reflected short-wave radiation. A deeper understanding requires information on the complete 3-D radiation exchange between trees and fabricated structures. In this context, the combination of TST, meteorological observations and energy balance models like DART EB (Gastellu-Etchegorry 2008) can be helpful.

Spatial variability of soil moisture and atmospheric turbulence within the FOV can produce temperature differences because these factors are important drivers of the leaf energy balance. The first aspect is beyond the scope of the study. Regarding the second aspect, Christen et al. (2011) showed that temperature fluctuations caused by atmospheric turbulence are spatially coherent and reveal the form of individual crowns. Conifers show a slightly lower spatial coherence than deciduous trees.

5 Conclusions

Our results illustrate that canopy temperature of urban trees depends on species-specific properties and the location of the tree. Moreover, the study shows that despite a distinct hot and dry period, the observed mature trees remain relatively cool in contrast to impervious surfaces. Knowledge of species-specific canopy temperature and the impacts of urban structures on the energy and water balance of trees is essential to optimise urban climates, e.g. to tackle adverse effects of the urban heat island. However, any advice for urban planning purposes depends on the climatological impacts you would like to have or not. Species with a lower canopy temperature like *P. nigra*, *Q. robur* or *Tilia cordata* are suitable for the reduction of air temperature. However, *Q. robur* and several species of *Populus* as well as *P. acerifolia* have a high ozone formation potential because of high emissions of volatile organic compounds (VOC) (Benjamin and Winer 1998). On the other hand, species with higher canopy temperatures like *A. platanoides* emit less VOC (Kesselmeier and Staudt 1999). A comprehensive evaluation and optimisation of benefits from urban trees should take the full range of climatological effects into account. These include the modification of surface temperature underneath trees, air quality, human thermal comfort, the ventilation of street canyons and the energy consumption of buildings.

Acknowledgments We would like to thank Petra Grasse (Institute of Meteorology, Freie Universität Berlin) for providing the cloud data and Jörn Welsch (Urban and Environmental Information System, Senate Department for Urban Development) for providing the impervious soil coverage map for Berlin. Especially we would like to thank Albert Polze, Britta Jänicke and Marco Otto for assistance in tree data collection and analysis.

References

Akbari H, Pomerantz M, Taha H (2001) Cool surfaces and shade trees to reduce energy use and improve air quality in urban areas. Sol Energy 70:295–310

Benjamin M, Winer A (1998) Estimating the ozone-forming potential of urban trees and shrubs. Atmos Environ 32:53–68

Bowler DE, Buyung-Ali L, Knight TM, Pullin AS (2010) Urban greening to cool towns and cities: a systematic review of the empirical evidence. Landscape Urban Plan 97:147–155

Brown R, Gillespie T (1990) Estimating radiation received by a person under different species of shade trees. J Arboric 16:158–161

Campbell GS, Norman JM (1998) An introduction to environmental biophysics. Springer, New York

Celestian SB, Martin CA (2005) Effects of parking lot location on size and physiology of four southwest landscape trees. J Arboric 31:191–197

Chmielewski FM, Köhn W (1999) The long-term agrometeorological field experiment at Berlin-Dahlem, Germany. Agric For Meteorol 96:39–48

Christen A, Meier F, Scherer D (2011) High-frequency fluctuations of surface temperatures in an urban environment. Theor Appl Climatol. doi:10.1007/s00704-011-0521-x

Elias P (1979) Leaf diffusion resistance pattern in an Oak-Hornbean forest. Biol Plantarum 21:1–8

Fortunati A, Barta C, Brilli F, Centritto M, Zimmer I, Schnitzler JP, Loreto F (2008) Isoprene emission is not temperature-dependent during and after severe drought-stress: a physiological and biochemical analysis. Plant J 55:687–697

Foster JR (1992) Photosynthesis and water relations of the floodplain tree, boxelder (Acer negundo L.). Tree Physiol 11:199–149

Fuchs M (1990) Infrared measurement of canopy temperature and detection of plant water stress. Theor Appl Climatol 42:253–261

Gastellu-Etchegorry J (2008) 3D modeling of satellite spectral images, radiation budget and energy budget of urban landscapes. Meteorol Atmos Phys 102:187–207

Grace J (1978) The turbulent boundary layer over a flapping Populus leaf. Plant Cell Environ 1:35–38

Grimmond CSB, Souch C, Hubble MD (1996) Influence of tree cover on summertime surface energy balance fluxes, San Gabriel Valley, Los Angeles. Clim Res 6:45–57

Gromke C, Ruck B (2007) Influence of trees on the dispersion of pollutants in an urban street canyon—experimental investigation of the flow and concentration field. Atmos Environ 41:3387–3302

Gulyás Á, Unger J, Matzarakis A (2006) Assessment of the microclimatic and human comfort conditions in a complex urban environment: modelling and measurements. Build Environ 41:1713–1722

Hagishima A, Narita K, Tanimoto J (2007) Field experiment on transpiration from isolated urban plants. Hydrol Processes 21:1217–1222

Handa IT, Körner C, Hattenschwiler S (2005) A test of the tree-line carbon limitation hypothesis by in situ CO2 enrichment and defoliation. Ecology 86:1288–1300

Heilman JL, Brittin CL, Zajicek JM (1989) Water-use by shrubs as affected by energy exchange with building walls. Agric For Meteorol 48:345–357

Heisler GM (1986) Effects of individual trees on the solar radiation climate of small buildings. Urban Ecol 9:337–359

Hoyano A (1988) Climatological uses of plants for solar control and the effects on the thermal environment of a building. Energy Build 11:181–199

Hoyano A, Asano K, Kanamaru T (1999) Analysis of the sensible heat flux from the exterior surface of buildings using time sequential thermography. Atmos Environ 33:3941–3951

Jones HG (1992) Plants and microclimate. Cambridge University Press, Cambridge

Kesselmeier J, Staudt M (1999) Biogenic volatile organic compounds (VOC): an overview on emission, physiology and ecology. J Atmos Chem 33:23–88

Kjelgren R, Montague T (1998) Urban tree transpiration over turf and asphalt surfaces. Atmos Environ 32:35–41

Körner C, Scheel JA, Bauer H (1979) Maximum leaf diffusive conductance in vascular plants. Photosynthetica 13:45–82

Lagouarde JP, Ballans H, Moreau P, Guyon D, Coraboeuf D (2000) Experimental study of brightness surface temperature angular variations of maritime pine (*Pinus pinaster*) stands. Remote Sens Environ 72:17–34

Lebourgeois F, Levy G, Aussenac G, Clerc B, Willm F (1998) Influence of soil drying on leaf water potential, photosynthesis, stomatal conductance and growth in two black pine varieties. Ann Sci Forest 55:287–299

Leuzinger S, Körner C (2007) Tree species diversity affects canopy leaf temperatures in a mature temperate forest. Agric For Meteorol 146:29–37

Leuzinger S, Vogt R, Körner C (2010) Tree surface temperature in an urban environment. Agric For Meteorol 150:56–62

Lindberg F, Grimmond C (2011) The influence of vegetation and building morphology on shadow patterns and mean radiant temperatures in urban areas: model development and evaluation. Theor Appl Climatol 105:311–323

Litschke T, Kuttler W (2008) On the reduction of urban particle concentration by vegetation—a review. Meteorol Z 17:229–240

Lusk CH, Wright I, Reich PB (2003) Photosynthetic differences contribute to competitive advantage of evergreen angiosperm trees over evergreen conifers in productive habitats. New Phytol 160:329–336

Mayer H, Höppe P (1987) Thermal comfort of man in different urban environments. Theor Appl Climatol 38:43–49

Meier F, Scherer D, Richters J (2010) Determination of persistence effects in spatio-temporal patterns of upward long-wave radiation flux density from an urban courtyard by means of Time-Sequential Thermography. Remote Sens Environ 114:21–34

Meier F, Scherer D, Richters J, Christen A (2011) Atmospheric correction of thermal-infrared imagery of the 3-D urban environment acquired in oblique viewing geometry. Atmos Meas Tech 4:909–922. doi:10.5194/amt-4-909-2011

Montague T, Kjelgren R (2004) Energy balance of six common landscape surfaces and the influence of surface properties on gas exchange of four containerized tree species. Sci Hortic 100:229–249

Morecroft MD, Roberts JM (1999) Photosynthesis and stomatal conductance of mature canopy Oak (Quercus robur) and Sycamore (Acer pseudoplatanus) trees throughout the growing season. Funct Ecol 13:332–342

Mueller EC, Day TA (2005) The effect of urban ground cover on microclimate, growth and leaf gas exchange of oleander in Phoenix, Arizona. Int J Biometeorol 49:244–255

Oke T (1979) Advectively-assisted evapotranspiration from irrigated urban vegetation. Bound-Lay Meteorol 17:167–173

Oke TR (1989) The micrometeorology of the urban forest. Philos Trans R Soc London, Ser B 324:335–349

Potchter O, Cohen P, Bitan A (2006) Climatic behavior of various urban parks during hot and humid summer in the Mediterranean city of Tel Aviv, Israel. Int J Climatol 26:1695–1711

Robitu M, Musy M, Inard C, Groleau D (2006) Modeling the influence of vegetation and water pond on urban microclimate. Sol Energy 80:435–447

Rosenfeld AH, Akbari H, Bretz S, Fishman BL, Kurn DM, Sailor D, Taha H (1995) Mitigation of urban heat islands—materials, utility programs, updates. Energy Build 22:255–265

Running SW (1976) Environmental control of leaf water conductance in conifers. Can J Forest Res 6:104–112

Sandford AP, Jarvis PG (1986) Stomatal responses to humidity in selected conifers. Tree Physiol 2:89–103

Schuepp PH (1993) Tansley review No. 59. Leaf boundary-layers. New Phytol 125:477–507

Senate Department for Urban Development (2007) Berlin digital environmental atlas 01.02 impervious soil coverage (sealing of soil surface). Database: Urban and Environmental Information System (UEIS). http://www.stadtentwicklung.berlin.de/umwelt/umweltatlas/e_text/ekb102.pdf. Accessed 21 Mar 2012

Shashua-Bar L, Hoffman ME (2000) Vegetation as a climatic component in the design of an urban street—an empirical model for predicting the cooling effect of urban green areas with trees. Energy Build 31:221–235

Shashua-Bar L, Pearlmutter D, Erell E (2009) The cooling efficiency of urban landscape strategies in a hot dry climate. Landscape Urban Plan 92:179–186

Souch CA, Souch C (1993) The effect of trees on summertime below canopy urban climates: a case study. Bloomington, Indiana. J Arboric 19:303–312

Spronken-Smith RA, Oke TR (1998) The thermal regime of urban parks in two cities with different summer climates. Int J Remote Sens 19:2085–2104

Streiling S, Matzarakis A (2003) Influence of single and small clusters of trees on the bioclimate of a city: a case study. J Aboric 29:309–316

Thorsson S, Lindqvist M, Lindqvist S (2004) Thermal bioclimatic conditions and patterns of behaviour in an urban park in Göteborg, Sweden. Int J Biometeorol 48:149–156

Upmanis H, Eliasson I, Lindqvist S (1998) The influence of green areas on nocturnal temperatures in a high latitude city (Göteborg, Sweden). Int J Climatol 18:681–700

Vogel S (2009) Leaves in the lowest and highest winds: temperature, force and shape. New Phytol 183:13–26

Voogt JA, Oke TR (1997) Complete urban surface temperatures. J Appl Meteorol 36:1117–1132

Voogt JA, Oke TR (2003) Thermal remote sensing of urban climates. Remote Sens Environ 86:370–384

Whitlow TH, Bassuk NL, Reichert DL (1992) A 3-year study of water relations of urban street trees. J Appl Ecol 29:436–450